

TECHNICAL REPORT ARCCB-TR-96023

ELEVATED TEMPERATURE PROPERTIES OF STEELS

G. N. VIGILANTE
A. FISH
G. P. O'HARA
D. CRAYON
T. HICKEY

19961113 138

AUGUST 1996



**US ARMY ARMAMENT RESEARCH,
DEVELOPMENT AND ENGINEERING CENTER**
CLOSE COMBAT ARMAMENTS CENTER
BENÉT LABORATORIES
WATERVLIET, N.Y. 12189-4050



APPROVED FOR PUBLIC RELEASE; DISTRIBUTION UNLIMITED

DTIC QUALITY INSPECTED 3

DISCLAIMER

The findings in this report are not to be construed as an official Department of the Army position unless so designated by other authorized documents.

The use of trade name(s) and/or manufacturer(s) does not constitute an official indorsement or approval.

DESTRUCTION NOTICE

For classified documents, follow the procedures in DoD 5200.22-M, Industrial Security Manual, Section II-19 or DoD 5200.1-R, Information Security Program Regulation, Chapter IX.

For unclassified, limited documents, destroy by any method that will prevent disclosure of contents or reconstruction of the document.

For unclassified, unlimited documents, destroy when the report is no longer needed. Do not return it to the originator.

REPORT DOCUMENTATION PAGE

Form Approved
OMB No. 0704-0188

Public reporting burden for this collection of information is estimated to average 1 hour per response, including the time for reviewing instructions, searching existing data sources, gathering and maintaining the data needed, and completing and reviewing the collection of information. Send comments regarding this burden estimate or any other aspect of this collection of information, including suggestions for reducing this burden, to Washington Headquarters Services, Directorate for Information Operations and Reports, 1215 Jefferson Davis Highway, Suite 1204, Arlington, VA 22202-4302, and to the Office of Management and Budget, Paperwork Reduction Project (0704-0188), Washington, DC 20503.

1. AGENCY USE ONLY (Leave blank)		2. REPORT DATE August 1996		3. REPORT TYPE AND DATES COVERED Final	
4. TITLE AND SUBTITLE ELEVATED TEMPERATURE PROPERTIES OF STEELS				5. FUNDING NUMBERS AMCMS No. 6226.24.H180.0 PRON No. TU5B5F261ABJ	
6. AUTHOR(S) G.N. Vigilante, A. Fish, G.P. O'Hara, D. Crayon, and T. Hickey					
7. PERFORMING ORGANIZATION NAME(S) AND ADDRESS(ES) U.S. Army ARDEC Benet Laboratories, AMSTA-AR-CCB-O Watervliet, NY 12189-4050				8. PERFORMING ORGANIZATION REPORT NUMBER ARCCB-TR-96023	
9. SPONSORING / MONITORING AGENCY NAME(S) AND ADDRESS(ES) U.S. Army ARDEC Close Combat Armaments Center Picatinny Arsenal, NJ 07806-5000				10. SPONSORING / MONITORING AGENCY REPORT NUMBER	
11. SUPPLEMENTARY NOTES Presented at the ASME/ICPVT Pressure Vessels and Piping Conference, Montreal, Quebec, Canada, 21-26 July 1996. Published in proceedings of the conference.					
12a. DISTRIBUTION / AVAILABILITY STATEMENT Approved for public release; distribution unlimited.				12b. DISTRIBUTION CODE	
13. ABSTRACT (Maximum 200 words) ASTM A723 and D6AC gun steels were evaluated for various high-temperature physical and mechanical properties, including specific heat, thermal expansion, stress relaxation, tensile, Young's modulus, and Poisson's ratio. Most tests were conducted at ambient temperature, 200°C, 300°C, and 400°C. A creep law was generated from the stress relaxation data that predicted the amount of creep strain at a given temperature as a function of stress and time. These data can be used, for example, to predict the amount of autofrettage stress lost at elevated temperatures and to establish safe gun tube service lives for various firing scenarios.					
14. SUBJECT TERMS Elevated Temperature Testing, Mechanical Properties, Physical Properties, Steels, Stress Relaxation, Creep				15. NUMBER OF PAGES 28	
				16. PRICE CODE	
17. SECURITY CLASSIFICATION OF REPORT UNCLASSIFIED	18. SECURITY CLASSIFICATION OF THIS PAGE UNCLASSIFIED	19. SECURITY CLASSIFICATION OF ABSTRACT UNCLASSIFIED	20. LIMITATION OF ABSTRACT UL		

TABLE OF CONTENTS

ACKNOWLEDGEMENTS	ii
EXECUTIVE SUMMARY	1
INTRODUCTION	1
EXPERIMENTAL PROCEDURE	2
Physical Property Tests	2
Mechanical Property Tests	3
RESULTS AND DISCUSSION	5
Physical Property Tests	5
Mechanical Property Tests	6
RECOMMENDATIONS/LESSONS LEARNED	8
Physical Property Tests	8
Mechanical Property Tests	8
REFERENCES	10

LIST OF TABLES

Table 1 Property data on candidate tube materials	11
Table 2 Typical chemical composition (wt%) of A723 and D6AC steels	12
Table 3 Elevated temperature tensile tests conducted on A723 and D6AC	12
Table 4 Stress relaxation of A723 and D6AC	13
Table 5 A723 Creep law coefficients and material constants	13
Table 6 UTS as a function of temperature and stroke rate for A723 and D6AC	13

LIST OF FIGURES

Figure 1	Schematic of strain-gaged specimen used for Young's modulus and Poisson's ratio tests	14
Figure 2	Schematic of operation for the Dynamic Mechanical Analyzer	15
Figure 3	Schematic of stress relaxation tests conducted using the Mandrel Method	16
Figure 4	Schematic of tensile tests conducted on the Gleeble	17
Figure 5	Thermal expansion coefficient	18
Figure 6	Young's modulus as a function of temperature for various steels	19
Figure 7	Poisson's Ratio vs. temperature for A723 and D6AC	20
Figure 8	Stress relaxation of A723	21
Figure 9	Stress relaxation of D6AC	22
Figure 10	Stress relaxed as predicted by creep model	23
Figure 11	Creep deflection vs. applied stress	24
Figure 12	Strength vs. temperature	25
Figure 13	Effects of loading rate and temperature on strength	26

Acknowledgements: The authors would like to thank Dan Corrigan for his assistance with the setup of the high-temperature strain gages, and John Underwood and Ed Troiano for their valuable insight and recommendations.

EXECUTIVE SUMMARY

This technical report details the physical and mechanical property tests conducted on ASTM A723 Grade 1 and D6AC high-strength steels at elevated temperature to be used in gun tube thermal management. The following is a synopsis of all tests conducted and the results obtained:

- **Specific Heat** - Specific heat results for both A723 and D6AC were suspect due to false peaks in the data; therefore, no results are presented in this report.
- **Thermal Expansion Coefficient** - The thermal expansion coefficient for A723 and D6AC increased logarithmically with increasing temperature which is consistent with previous test data.
- **Stress Relaxation Tests** - At temperatures ranging from 200°-450°C, exposure times of two and four hours, and at stress levels of 550 MPa and 850 MPa, A723 consistently exhibited more stress relaxation than D6AC. For the most severe test conditions, the stress relaxed in A723 was approximately 200 MPa, twice that of D6AC.

A creep law was developed for A723 using the stress relaxation data.

- **Elevated Temperature Tensile Tests** - The 0.1% yield strength and ultimate tensile strength at conventional testing stroke rates were consistent with published data. At 400°C, A723 lost approximately 20% of its room temperature strength. At very high stroke rates, the yield strength approached the ultimate tensile strength.
- **Young's Modulus** - Young's modulus tests using high-temperature strain gages provided scattered results; however, a general trend of decreasing Young's modulus with increasing temperature was observed.

The Dynamic Mechanical Analyzer method measured Young's modulus continually with temperature and showed a decrease with increasing temperature similar to that from the strain gage data. Once properly calibrated, the dynamic method proved to be a much more convenient and accurate test than strain gage method.

- **Poisson's Ratio** - Poisson's ratio tests using high temperature strain gages provided mixed results, though a decreasing trend with increasing temperature was observed.

INTRODUCTION

Gun tube thermal management is essential in determining the effects of rapid fire scenarios on the physical and mechanical properties of cannon tube materials. For example, stress relaxation may occur, ultimately leading to loss of desirable compressive autofrettage stresses at the bore surface which, in turn, can result in lowered fatigue life and bore closure.

Early in this test program, candidate steels, in addition to A723, were identified for service at elevated temperatures. An evaluation matrix (see Table 1) was established using criteria such as yield strength at elevated temperatures, room temperature fracture toughness, and ease of chromium plating or "platability" (a constant concern for our applications).

Two materials in Table 1, AF1410 and 1CR-Mo-V, were provisionally ruled out as potential gun tube materials due to their inherent properties, which are highlighted.

After discussion with ARDEC experts in materials, producibility, and plating, we proceeded with D6AC, similar in chemistry to A723 (Table 2) with the exception of slightly higher carbon and molybdenum for elevated temperature strength. D6AC is a high-temperature Cr-Mo-V steel currently used in some gun tube applications. The use of D6AC is for comparative purposes and does not suggest that D6AC is the only potential replacement material for A723, but rather gives beneficial information on a widely used high-temperature steel.

The objectives of the project were to:

- Identify alternative high-strength steels to operate in elevated temperatures
- Determine the elevated temperature properties of gun steel (ASTM A723 Grade 1) at temperatures up to 450°C in order to predict the residual stress losses in the gun tube resulting from rapid fire scenarios
- Increase the accuracy of physical and mechanical property data on A723 for finite element modeling.

EXPERIMENTAL PROCEDURE

All materials used for this investigation were taken from existing gun tubes. The D6AC material was reheat-treated to increase its strength. All D6AC specimens were taken in the longitudinal or axial orientation because of wall thickness limitations. When possible, all test samples from both materials were taken from mid-wall locations.

Physical Property Tests

Thermal Expansion Coefficient

Thermal expansion coefficient is an important physical property that can be used to predict the deflection of the gun tube caused by thermal gradients. In this study, we measured the instantaneous thermal expansion coefficient using a dual-rod dilatometer with a fused silica reference. The thermal expansion coefficient is defined as:

$$\alpha = \frac{\Delta l / l_o}{\Delta T} \quad (1)$$

where Δl is the length change, l_o is the length at the reference temperature, and ΔT is the change in temperature. In a standard dilatometer, the actual coefficient of thermal expansion is the sum of the apparent expansion and the expansion contribution of the measuring system. A dual-rod dilatometer overcomes the problem of finding the system contribution by measuring the difference in expansion between the sample and a reference, using the same measuring apparatus.

The A723 and D6AC samples were taken from the longitudinal direction. The data were collected from room temperature to 650°C at a heating rate of 2°C/min. The system had an inert purified helium purge during testing to prevent oxidation from occurring.

Specific Heat

Specific heat, C_p , by definition is the amount of energy required to raise 1 gram of material, 1° C. Thus, C_p provides valuable information for the thermal modeling of cannon firings. The heat capacity measurements were performed with a differential scanning calorimeter (DSC). The DSC measures the differential heat flow between the sample and reference during thermal cycling. Approximately 20 mg of A723 and D6AC were needed for each test run.

Mechanical Property Tests

Young's Modulus

Young's modulus, also known as the elastic modulus in tension, is defined as:

$$E = \sigma_e / e_e \quad (2)$$

where σ_e is the elastic stress and e_e is the elastic strain. At elevated temperatures Young's modulus decreases in value, resulting in loss of stiffness of the cannon and increased muzzle droop.

Young's modulus was tested on both materials using two methods. The first method used high-temperature strain gages in uniaxial tension using an Instron Mechanical Tester. Conventional strain gages which utilize an adhesive interface, have a maximum operating temperature of only approximately 230°C; therefore, weldable gages having a maximum operating temperature of 1,090°C were used. These gages were adhesively bonded to a steel shim with a ceramic cement, which in turn was attached to the specimen by capacitive discharge spot welding. A forced hot air oven was attached to the Instron for the elevated temperature tests. To compensate for temperature effects, a half-bridge strain gage circuit was used. This incorporated one "dummy" gage for each "active" gage and compensated for thermal expansion effects in the specimen. The specimen configuration and strain gage location are shown in Figure 1. The test specimen used was of rectangular cross-section containing one longitudinal gage. No significant off-axis alignment was detected in the test fixture, justifying the use of only one longitudinal gage. Strain readings were recorded at various load levels. At the highest load level, the test specimen was at approximately one half of its yield strength to avoid microplasticity. Because we were well within the elastic limit of the test specimen, only one or two specimens were used for each material tested. The longitudinal strain was recorded at each load level. The load was removed and reloaded, and the longitudinal strain recorded again to ensure repeatability.

Young's modulus was also measured using a dynamic method. The Dynamic Mechanical Analyzer (DMA) operates on the principle of forced resonant vibration at a user-defined oscillation amplitude. The electromagnetic driver displaces the arms as shown in Figure 2, which flexes the sample through a fixed deformation and resonates the system. The DMA records the frequency of oscillation and the electrical energy used by the driver to maintain the oscillation amplitude. Thin rectangular strips were cycled from room temperature to 450°C at a rate of 5°C/min. A nitrogen environment was used to eliminate oxidation of the sample and the system.

Poisson's Ratio

Poisson's ratio is defined as the ratio of the transverse strain to the longitudinal strain:

$$\nu = -\frac{e_t}{e_l} \quad (3)$$

The procedures used for Poisson's ratio tests were identical to those used for Young's modulus tests using elevated temperature strain gages. No significant off-axis alignment was detected in the test fixture justifying the use of one longitudinal gage and one transverse gage.

Stress Relaxation Testing

As previously mentioned, stress relaxation and creep are critical for determining the loss of residual stresses in the cannon at elevated temperatures. Stress relaxation tests were conducted using the mandrel method described in ASTM E328 and by Underwood et al.⁽¹⁾ Figure 3 shows a schematic of the stress relaxation tests conducted. Test specimens 0.1" thick were clamped over mandrels of 475 mm and 307 mm radii to produce elastic outer fiber stresses of 550 MPa and 850 MPa, respectively. These two stress levels were in the range of typical autofrettage stresses in cannon. The elastic outer fiber stress in the test specimens was calculated by the following equation:

$$\sigma_{applied} = E \left[\frac{h/2}{R_m + h/2} \right] \quad (4)$$

where E is Young's modulus, h is the thickness, and R_m is the radius of the mandrel. All tests were conducted at temperatures ranging from 200°-450°C for two and four hours. These two times were consistent with the times used in the post-autofrettage heat treatment and were used to establish the time dependence of creep for both materials. After the tests were conducted, the permanent deflection of the specimens was measured to the nearest 0.0025 mm using a machinist microscope. The radius of curvature of the test specimens, R_s , was calculated from the measured deflection using a geometric expression. R_s was substituted for R_m in equation (4) to calculate stress relaxation.

The data from all stress relaxation tests on A723 and D6AC were presented to the Modeling and Simulation Branch, Benét Laboratories, to analyze and generate a creep law.

Elevated Temperature Stress/Strain Tests

This investigation was designed to determine the effects of elevated temperature and stroke rate on the yield strength (YS) and ultimate tensile strength (UTS) of A723 and D6AC. A Gleeble 1500 Thermal Mechanical Testing System was used for all tests. The Gleeble 1500 is designed to perform a variety of tests, including compression, hot compression, hot ductility, weldability studies, tensile, and fatigue. The experiments conducted on A723 and D6AC used the high-temperature and stroke rate variation capabilities of the Gleeble 1500. The system can run either manually or automatically. In automatic control, a computer interfaces with the modules that manipulate the specimen during a test. The Gleeble 1500 has a maximum heating rate of more than 10,000°C/s for a 6-mm diameter plain carbon steel bar, with a 15-mm gage length,

using a 480 volt power line with a minimum 200 ampere supply. The maximum force in tension or compression is 80 kN. The maximum and minimum stroke rates are 1000 mm/s and 1.7×10^{-5} mm/s, respectively.

An attempt was made to heat-treat the D6AC material to a yield strength identical to the A723 material, which had an average room temperature yield strength of 1145 MPa. The resulting yield strength of the D6AC material was higher than projected (1343 MPa) most likely due to the more complex dual-step quenching and tempering of this alloy.

Thermal/mechanical testing was performed on both A723 and D6AC steels according to the test parameters shown in Table 3 and following ASTM E8 and ASTM E21 guidelines. For data comparison purposes, a minimum of three tensile specimens of each material was tested at each temperature.

The tensile bars were machined with threaded ends in order to be used with available test fixturing (Figure 4). After the original test plan was completed, additional tests were run at very high stroke rates to determine the yield strength increase.

The Gleeble 1500 Thermal Mechanical Testing System applies heat in the form of conduction, thereby minimizing the time for the tensile bar to reach the desired temperature. The strain was measured using a quartz C-strain measuring device, which monitors the crosswise strain of the tensile bar. On average, the tensile tests conducted at 0.013 mm/s were completed in less than eight minutes, and the tensile tests conducted at the 212 mm/s were completed in approximately 30 ms. The information generated from each test was downloaded to an ASCII file and converted to an Excel worksheet. The crosswise strain was converted to lengthwise strain using a Poisson's ratio of 0.285, a typical value for steels. Stress-time, strain-time, and stress-strain data were analyzed for all tests conducted and a stress vs. temperature plot generated for A723 and D6AC.

RESULTS AND DISCUSSION

Physical Property Tests

Specific Heat

The specific heat capacity results for both materials were suspect because a peak was observed at approximately 400°C. These peaks are commonly observed to coincide with phase changes in the material; however, no phase change occurs in A723 or D6AC at 400°C. The false peak may be attributed to improper calibration of the samples or to the presence of an artifact in the samples.

Thermal Expansion Coefficient

The thermal expansion coefficient for both alloys increased logarithmically with increasing temperature as seen in Figure 5. These results are slightly higher than that of Cox⁽²⁾ at test temperatures above 200°C. The differences between the two sets of data may be attributed to the significantly larger data set obtained in our tests.

Mechanical Property Tests

Young's Modulus

Young's modulus shows a definite downward trend with increasing temperature as reported in the literature. Figure 6 shows Young's modulus for both A723 and D6AC using both the strain gage and dynamic method. Also on this plot are the Young's modulus values measured by Barranco⁽³⁾ for AISI 4340 steel. Numerous samples were run using the dynamic method, which provided a statistically meaningful data set. Aberrant Young's modulus data using the dynamic method were found to be related to a failing mechanical component in the system, which was eliminated. The easy collection of numerous data points provides a distinct advantage to the less time-consuming DMA method.

Poisson's Ratio

Poisson's ratio was found to decrease with increasing temperature as seen in Figure 7. Figure 7 contains only the best data sets; it excludes those data obtained at low-load levels, those that did not correspond to known room temperature values, and those that did not return to near zero upon removal of the load. Because of the amount of scatter in the D6AC data, the data were incorporated into the A723 Poisson's ratio data, and a linear regression fit was made. The assumption that Poisson's ratio of D6AC and A723 are near identical is not unreasonable because of the similarity in chemical composition between the two alloys. From Figure 7, the room temperature Poisson's ratio was 0.316, slightly higher than the typical room temperature values of 0.285-0.300 for steels.

Although a definite trend of decreasing Poisson's ratio with increasing temperature was observed, the data were somewhat suspect. Caution should be taken if these values are to be used in mechanical analyses. The most obvious location for error was in the strain gages themselves. In addition to the $\pm 5\%$ inherent error in the gages, errors may have occurred due to the weight of the 1.5 m long rigid lead wires acting on the gage. The thermal currents generated in the large forced air furnace were another potential source of error.

Stress Relaxation Testing

The results from the mandrel tests clearly indicated that more stress was relaxed in A723 than D6AC, as seen in Figures 8 and 9. The data in Figures 8 and 9 were fitted with simple polynomial expressions with high-correlation coefficients and were intended only to show the trend in the stress relaxation data. For clarity, only the four-hour time exposures are shown (the two-hour data for both materials showed similar trends as the four-hour data). As expected, when the applied stress in the A723 and D6AC specimens was increased from 550 MPa to 850 MPa, the amount of stress relaxation increased. Likewise, as temperature increased, the amount of stress relaxation increased. A similar trend was observed with an increase in time, although to a much lesser extent. As the test temperature increased, much more scatter was observed with the A723 specimens due to accelerated creep effects. Similar scatter would be expected with D6AC at higher test temperatures. Table 4 indicates the approximate stress relaxation that occurred in A723 and D6AC with a four-hour exposure at 850 MPa. Note that under the most severe condition, 450°C, the stress relaxed in A723 was twice that of the D6AC. Though A723 and D6AC are similar steels, D6AC contains more C and Mo than A723. Both C and Mo are known to retard dislocation and grain boundary motion, two essential features of creep.

Creep Law

A creep law was developed based on the use of available analytical tools and data generated from the stress relaxation tests. ABAQUS finite element code was used in accordance with ASTM E328 to model the creep law. The built-in equation for the creep law is:

$$\text{Creep Rate} = \frac{d\epsilon}{dt} = A\sigma^n t^m \quad (5)$$

In this equation, the creep rate is a function of two basic parameters, the local equivalent stress (σ) and time (t). These are related by the experimental material parameters A , n , and m which are defined as a function of temperature. Because of the normal data scatter and limited size of the experimental data, the stress exponent n was taken as a constant 1.77. The change in time from two hours to four hours demonstrated almost no change in creep effect. The time exponent was set at -0.75 to reflect the almost negligible effect of time as compared with temperature. At 100°C, the creep was assumed to be essentially zero, which was supported by the stress relaxation data obtained at 200°C. Table 5 shows the coefficients and material constants used in the creep law.

Figure 10 shows the amount of stress relaxed in the mandrel bend specimens as predicted from the creep law for an applied outer fiber stress of 850 MPa over a range of temperatures and times. Figure 10 was generated by first integrating equation (5) and solving for the creep strain. The outer fiber stress relaxed was then calculated by multiplying by Young's modulus. This outer fiber stress relaxation was compared with the bulk stress relaxation from the mandrel bend specimens over various temperatures and scaled down accordingly to match the experimental data. This allowed us to extrapolate to short-time exposures. The points represent actual test data that were used to create the creep model, while the dashed lines represent extrapolation to shorter times. It must be understood that the extrapolated short-time stress relaxation data taken from equation (5) may not be representative of what actually occurs, since our tests were based on time exposures on the order of hours not minutes. Oehlert and Atrens⁽⁴⁾ recently found that creep can occur in high-strength steels similar to our gun steels at temperatures lower than 100°C, at stresses greater than 50% of the 0.2% YS, and for time durations on the order of minutes. Hence, stress relaxation from short-time durations may be significant and should be further investigated.

Figure 11 shows the creep deflection versus applied stress at temperatures ranging from 300°C to 450°C. The ABAQUS solutions agree well with the experimental data from the stress relaxation tests.

In the investigated temperature range, creep was a strong function of all three fundamental parameters: stress, temperature, and time. The creep data clearly showed greater than 10-fold increase in the creep stress between 300°C and 450°C. The data also demonstrated that the creep effect developed quickly in time; however, because of insufficient time data, detailed analysis on the time effect cannot be currently investigated.

Elevated Temperature Tensile Tests

The data generated by the Gleeble 1500 at conventional testing stroke rates, shown in Figure 12, indicated a reduction in strength with an increase in temperature of both A723 and D6AC. These data trends were consistent with the work performed by Underwood et al.,⁽¹⁾ on A723 and by Barranco⁽³⁾ on 4340 steel. The data indicated that the room temperature 0.1% YS properties of the D6AC material were 16% higher than the A723 material. The higher strength values of the D6AC material were not unexpected, since the

original heat treatment produced higher strength values than originally anticipated. All the results shown in this graph were based on data generated by longitudinally oriented tensile specimens for clarity and comparison purposes. The general trend of the graph indicates a decrease in strength with an increase in temperature.

The high stroke rate tests were performed on the longitudinally oriented A723 material, as shown in Figure 13. The UTS was the only discernible value that could be obtained from the results. The UTS was observed to be 1317 MPa, which is 64 MPa higher than the tests run at the much slower stroke rate. It should be noted from Barranco's data⁽³⁾ that as the stroke rate was increased, the 0.1% YS approached the UTS. Since our high stroke rate tests were over two orders of magnitude faster than Barranco's highest stroke rate, the YS for the A723 under dynamic conditions should approximate the UTS.

RECOMMENDATIONS/LESSONS LEARNED

Physical Property Tests

Specific Heat

- Test additional samples due to the suspect nature of the data obtained. Convert to a platinum reference and sample pans to extend the test temperature range and eliminate any question of boundary effects.

Thermal Expansion Coefficient

- Conduct additional runs to produce a statistically meaningful set of data. The thermal expansion measurements made with a dual-rod dilatometer were accurate and reproducible.

Mechanical Property Tests

Young's Modulus

- Use the DMA method due to the poor Young's modulus results obtained using high temperature strain gages for both materials. The test is much less labor-intensive, and time-consuming and can generate data continuously as the temperature is increased.
- If unfamiliar materials are being investigated, examine both the static method and dynamic method, at least at room temperature, to determine if significant deviations are present.

Poisson's Ratio

- Because of the difficulties in measuring transverse strain using high-temperature strain gages, calculate future Poisson's ratio tests from elastic moduli from the following expression:

$$\frac{E}{2G} - 1 = \nu \quad (6)$$

where E is Young's modulus and G is the shear modulus. These tests can be performed using either a high-temperature torsional extensometer or a DMA with the capability to measure in a shear/torsional mode. Unfortunately, our DMA cannot measure in this mode.

Stress Relaxation and Creep Analysis

- Investigate other high-temperature alloys, in addition to D6AC as candidate high-temperature gun tube materials. The slight compositional differences between A723 and D6AC had great impact on the amount of stress relaxed. For the temperature range examined in this experiment, D6AC showed much more resistance to stress relaxation than A723. Conduct typical mechanical property tests, including J_{IC} fracture toughness, producibility, and platability.
- Conduct additional tests to analyze the effects of short-exposure times on the stress relaxation of A723, since the stress relaxation and creep analysis did not address the "time at temperature" effect of short temperature pulses that occur during a gun firing. Recent work by Oehlert and Atrens⁽⁴⁾ indicates the significance of short-time exposures at low temperatures for high-strength steels.

Elevated Temperature Tensile Tests

- Though the amount of stress relaxed in A723 was significantly greater than D6AC at temperatures up to 450°C, the loss of tensile strength in D6AC seems to be very similar to that of A723.
- Conduct additional tests on A723 at temperatures up to the upper critical temperature (approx. 900°C) and at high stroke rates.
- Develop a similar quartz gage for the longitudinal direction to eliminate the problems encountered while measuring the crosswise strain (transverse strain) of the specimen.

REFERENCES

1. Underwood, J. H., Fujczak, R. R., and Hasenbein, R. G., "Elastic, Strength, and Stress Relaxation Properties of A723 Steel and 38644 Titanium for Pressure Vessel Applications," ARDEC Technical Report #88011, Benét Laboratories, Watervliet Arsenal, NY, March 1988.
2. Cox, J., Unpublished Research, Benét Laboratories, Watervliet, NY, Circa 1980.
3. Barranco, J. M., "Tensile Properties of Steel at Elevated Temperatures," WVT RR-5905, Watervliet Arsenal, Watervliet, NY, November 1959.
4. Oehlert, A., and Atrens, A. "Room Temperature Creep of High Strength Steels," Acta Met. Mater., Vol. 42, No. 5, 1994, pp. 1493-1508.

Table 1. Property data on candidate tube materials

Material	A723 Grade 1	D6AC	5Cr-Mo-V	200 Maraging	PH 13-8 Mo	AF1410	1Cr-Mo-V
Source of Info	MIL-S-46119B	Aero. Struc. Mat. Handbook	Aero. Struc. Mat. Handbook	Teledyne Vasco Product Lit. Aero. Struc. Mat. Handbook	Aero. Struc. Mat. Handbook	TR-91021 [Troiano]	ASTM A193/B16 MIL-S-46047E
Chemistry (wt%)	Fe-2Ni-1Cr- 5Mo-.35C-.1V	Fe-1Cr-1Mo- 5Ni-.45C-.1V	Fe-5Cr-1.3Mo- 5V-.4C	Fe-18Ni-8Co- 3Mo-.2Ti- .03Cmax	Fe-13Cr-8Ni- 2Mo-.1Al- .05Cmax	Fe-14Co-10Ni- 2Cr-1Mo-.16C	Fe-1Cr-1Mn- .6Mo-.4C-.25V
YS at RT; MPa [Ksi]	≈11,170 [170]	≈1,300 [190]	1,380 [200]	≈1,380 [200]	≈1,345 [195]	1,427 [207]	760 [110]
YS at 200°C MPa [Ksi]	≈1,120 [162]	≈1,140 [165]	1,268 [184]	≈1,254 [182]	≈1,207 [175]	1,317 [191]	
YS at 300°C MPa [Ksi]	≈1,067 [155]	≈1,035 [150]	1,197 [174]	≈1,214 [176]	≈1,138 [165]	1,134 [165]	
YS at 400°C MPa [Ksi]	≈1,015 [147]	≈900 [130]	1,123 [163]	≈1,145 [166]	≈1,089 [158]	1,007 [146]	
%RA	25 min.	50	≈40	≈55	≈52	67	45
CVN; J [ft-lb]	20 min. [15] at -40°		≈20 [15] at -40°	≈47 [15] at -40°	≈47 [35] at -40°		
Toughness at RT MPa√m [Ksi√in.]	≈121 [110]		≈111? [100]	≈121 [110]	≈144 [130]	≈174 [159]	
Formability	good		?				
Machinability	good		?			poor	
Platability	good				?		

Notes:

- All material properties are in S.I units; [] = English units.
- Shaded regions provisionally disqualify materials for use in this program
- 1Cr-Mo-V was excluded because of low strength
- AF1410 was excluded because of low strength at elevated temperatures and poor machinability.

Table 2. Typical chemical composition (wt%) of A723 and D6AC steels

Alloying Element (wt%)	A723 Grade 1		D6AC	
	Typical	ARDEC	Typical	ARDEC
Carbon (C)	.35 max	.33	.45-.50	.47
Nickel (Ni)	1.50-2.25	2.26	.40-.70	.65
Chromium (Cr)	.80-2.00	1.00	.90-1.20	1.03
Molybdenum (Mo)	.20-.40	.46	.90-1.10	1.06
Manganese (Mn)	.90 max	.69	.60-.90	.77
Vanadium (V)	.20 max	.09	.08-.15	.17
Copper (Cu)	-	-	.35 max	.07
Silicon (Si)	.35 max	.21	.15-.30	.27
Phosphorus (P)	.015 max	.006	.010 max	.011
Sulfur (S)	.015 max	.005	.010	.002
Iron (Fe)	Balance		Balance	

Table 3 - Elevated temperature tensile tests conducted on A723 and D6AC

Temperature (°C)	Material	Stroke Rate (mm/s)
22	A723, D6AC	0.013
22	A723	212
200	A723, D6AC	0.013
300	A723, D6AC	0.013
400	A723, D6AC	0.013
400	A723	212
511	D6AC	0.013

Table 4. Stress relaxation of A723 and D6AC

Material	Stress Relaxed (MPa) at Initial Stress of 850 MPa				
	200°C	300°C	350°C	400°C	450°C
A723	11	46	80	129	198
D6AC	16	40	56	76	99

Table 5 - A723 Creep law coefficients and material constants

Temp. (C)	A	n	m
100	1.00E-20	1.77	-0.75
300	1.10E-10	1.77	-0.75
350	2.94E-10	1.77	-0.75
400	6.71E-10	1.77	-0.75
450	12.41E-10	1.77	-0.75

Table 6. UTS as a function of temperature and stroke rate for A723 and D6AC

Material	Stroke Rate (mm/s)	UTS			
		22°C	200°C	300°C	400°C
A723	0.013	1,253	1,163	1,121	1,007
A723	212	1,317	No Result	No Result	1,092
D6AC	0.013	1,441	1,336	1,271	1,154
4340 ⁽³⁾	0.021	1,353	1,280	1,236	1,107
4340 ⁽³⁾	0.85	1,381	1,267	1,226	1,124

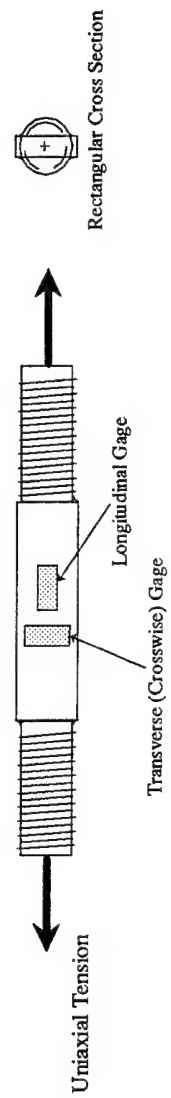


Figure 1. Schematic of strain-gaged specimen used for Young's modulus and Poisson's ratio tests

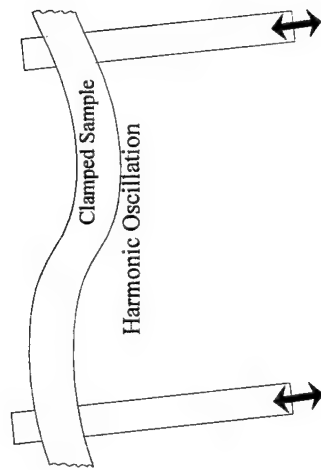


Figure 2. Schematic of operation for the Dynamic Mechanical Analyzer

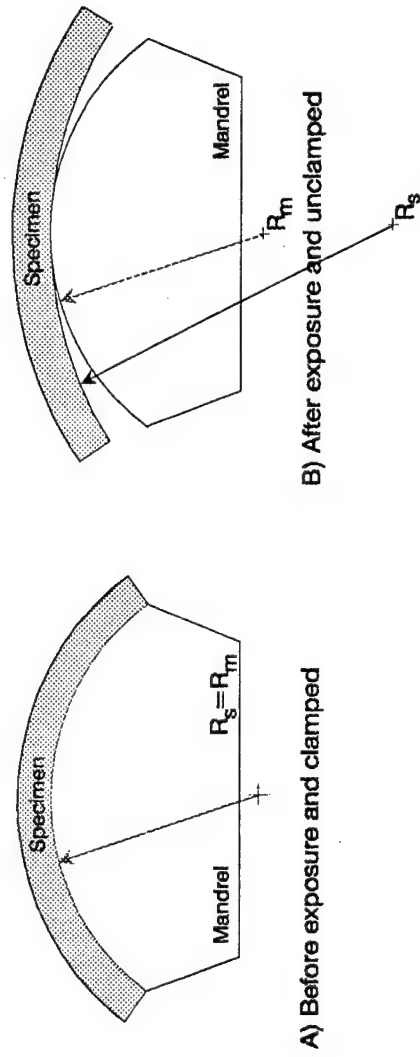


Figure 3. Schematic of stress relaxation tests conducted using the Mandrel Method

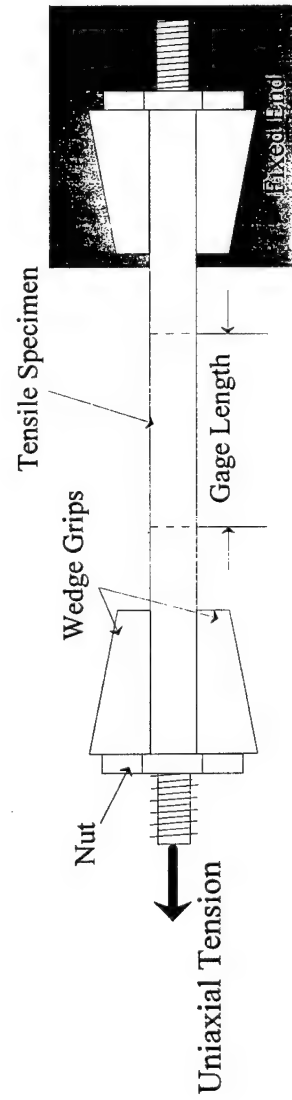


Figure 4. Schematic of tensile tests conducted on the Gleeble

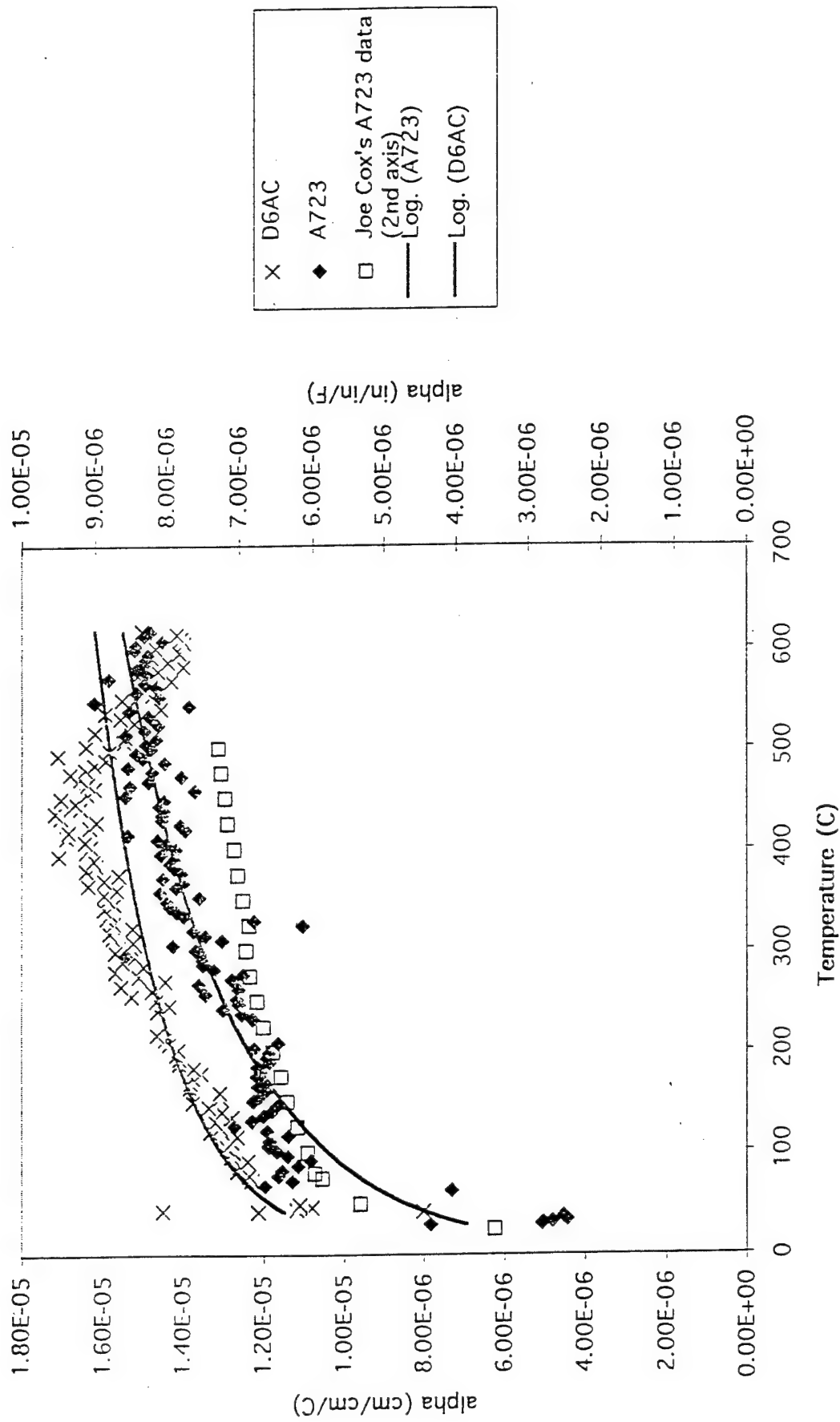


Figure 5. Thermal expansion coefficient

Temperature Dependence of the Modulus

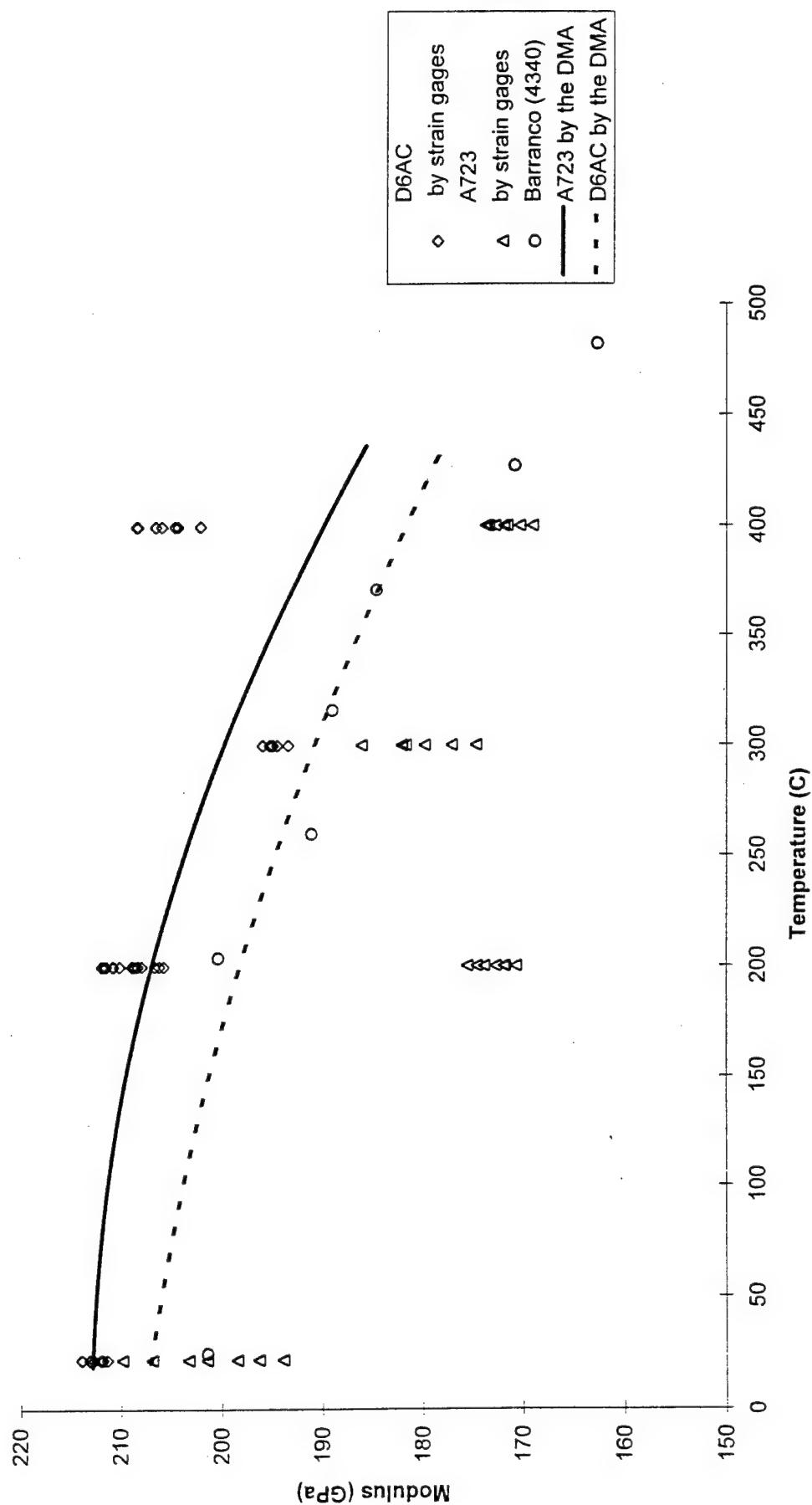


Figure 6. Young's modulus as a function of temperature for various steels

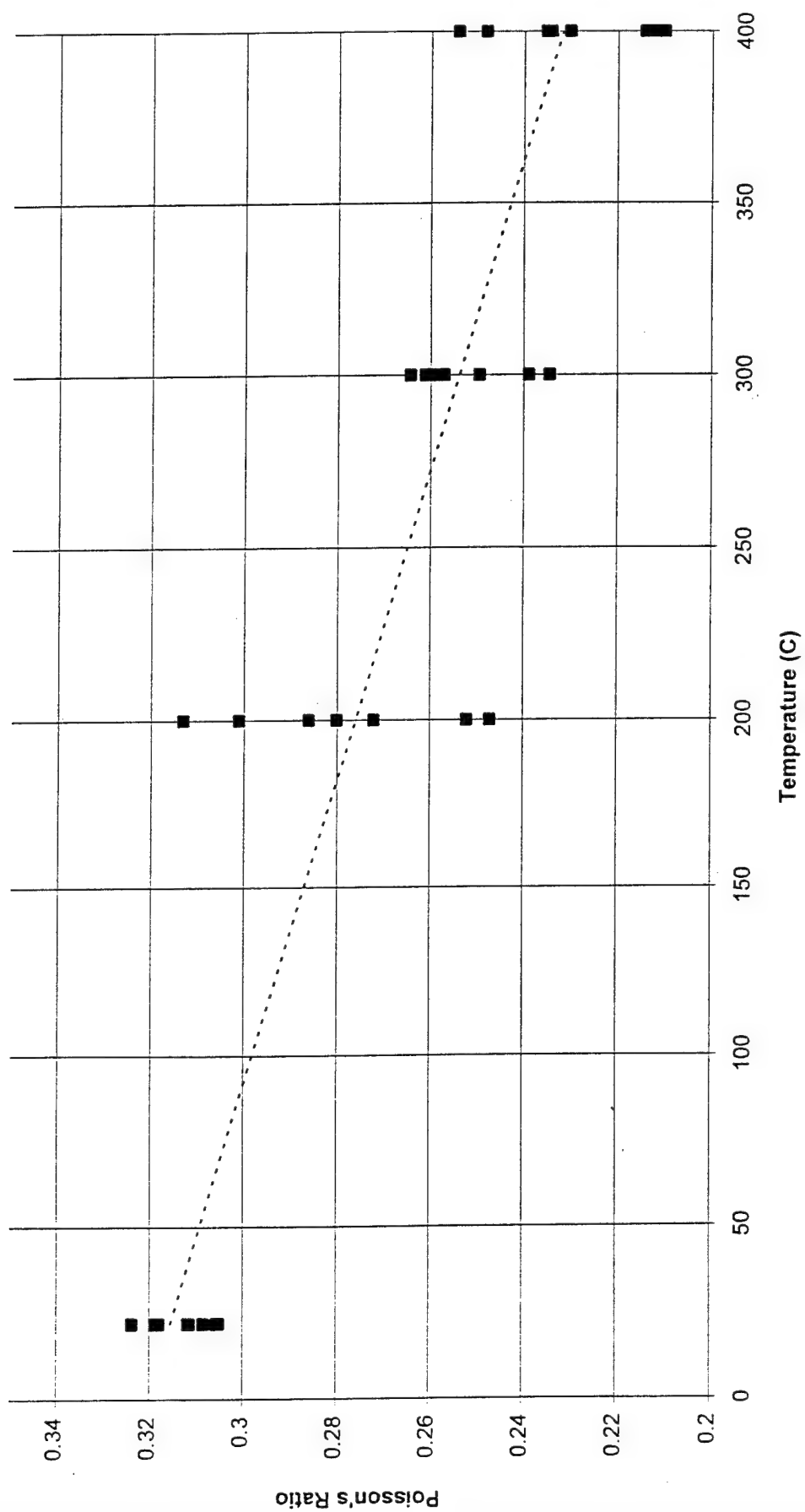


Figure 7. Poisson's Ratio vs. temperature for A723 and D6AC

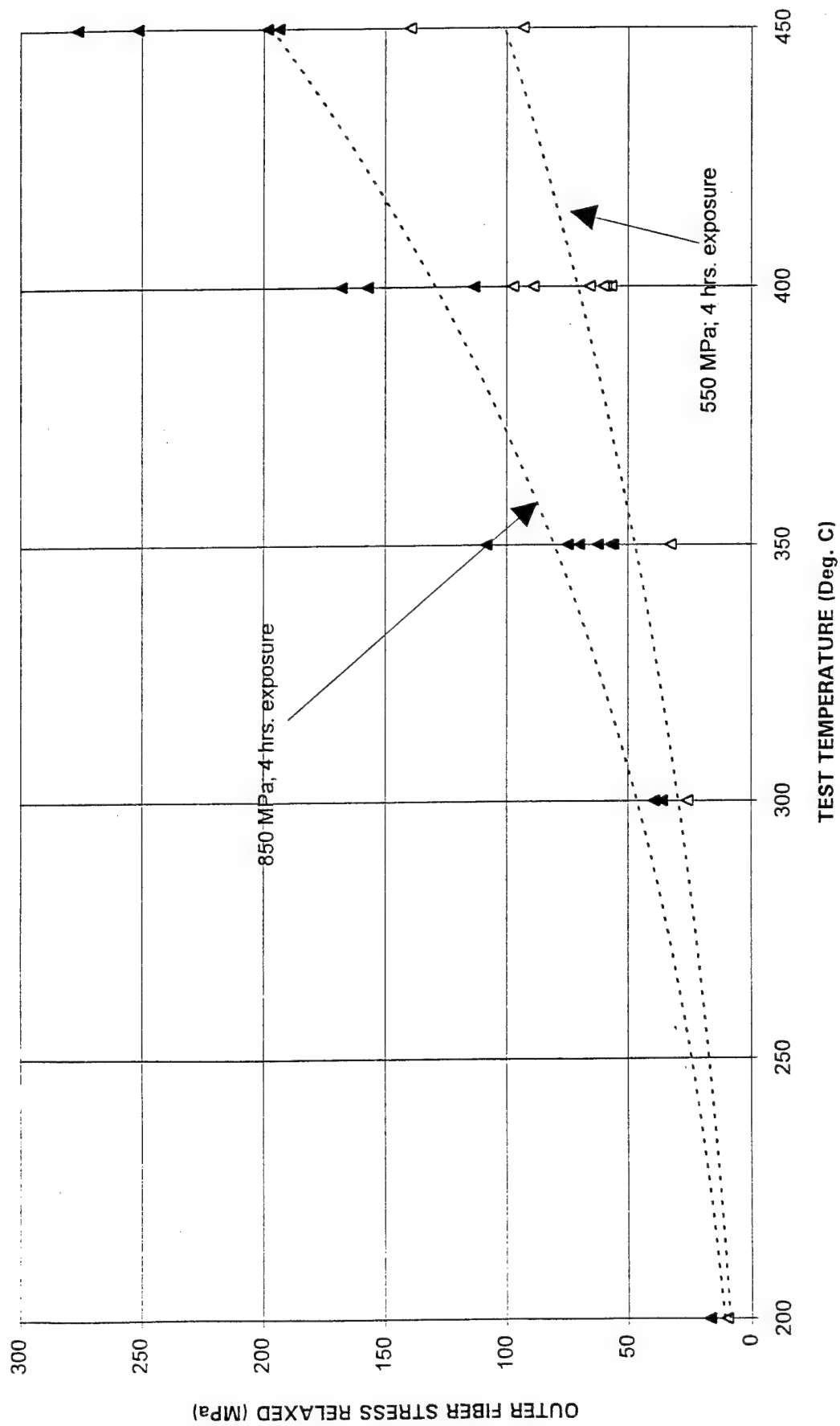


Figure 8. Stress relaxation of A723

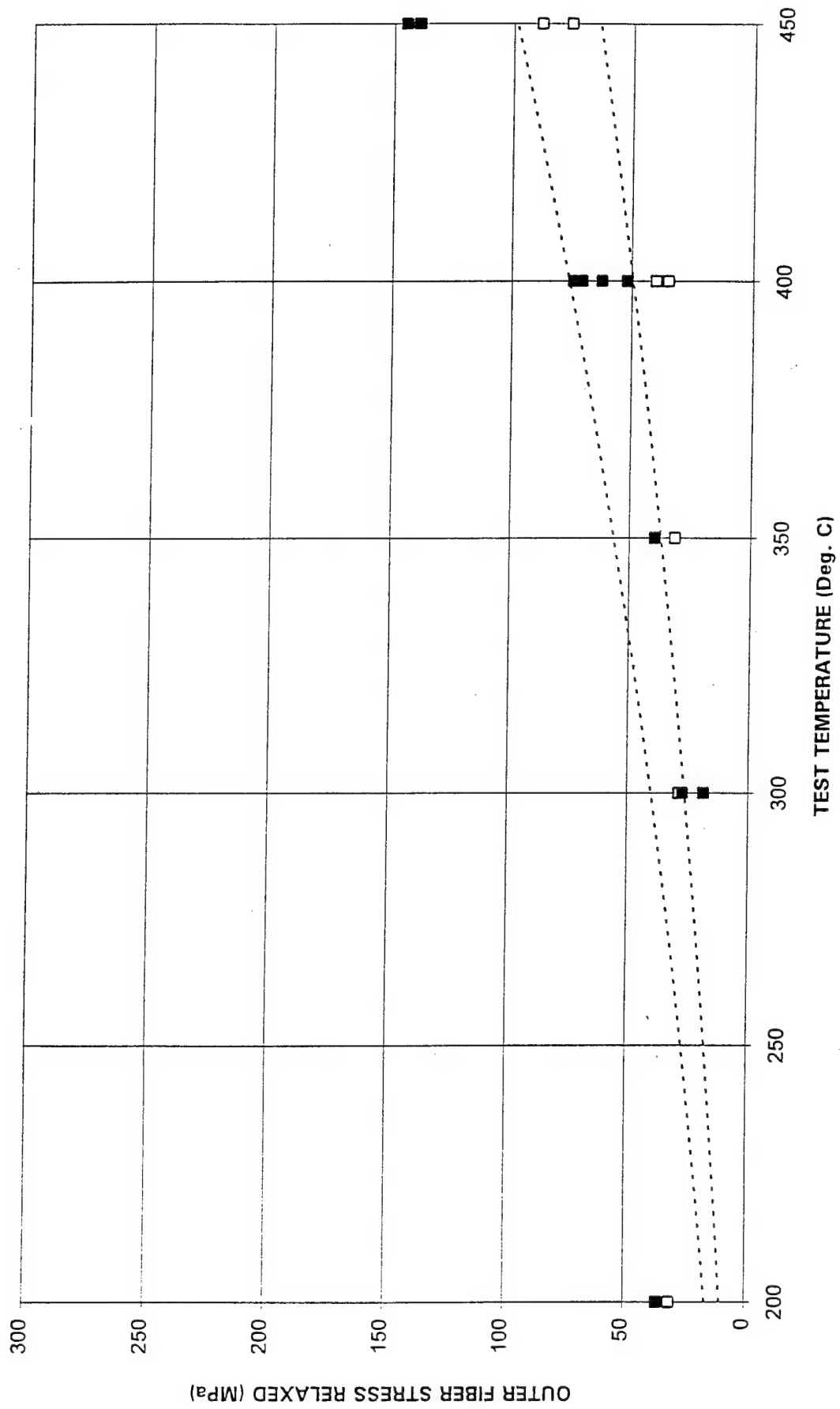


Figure 9. Stress relaxation of D6AC

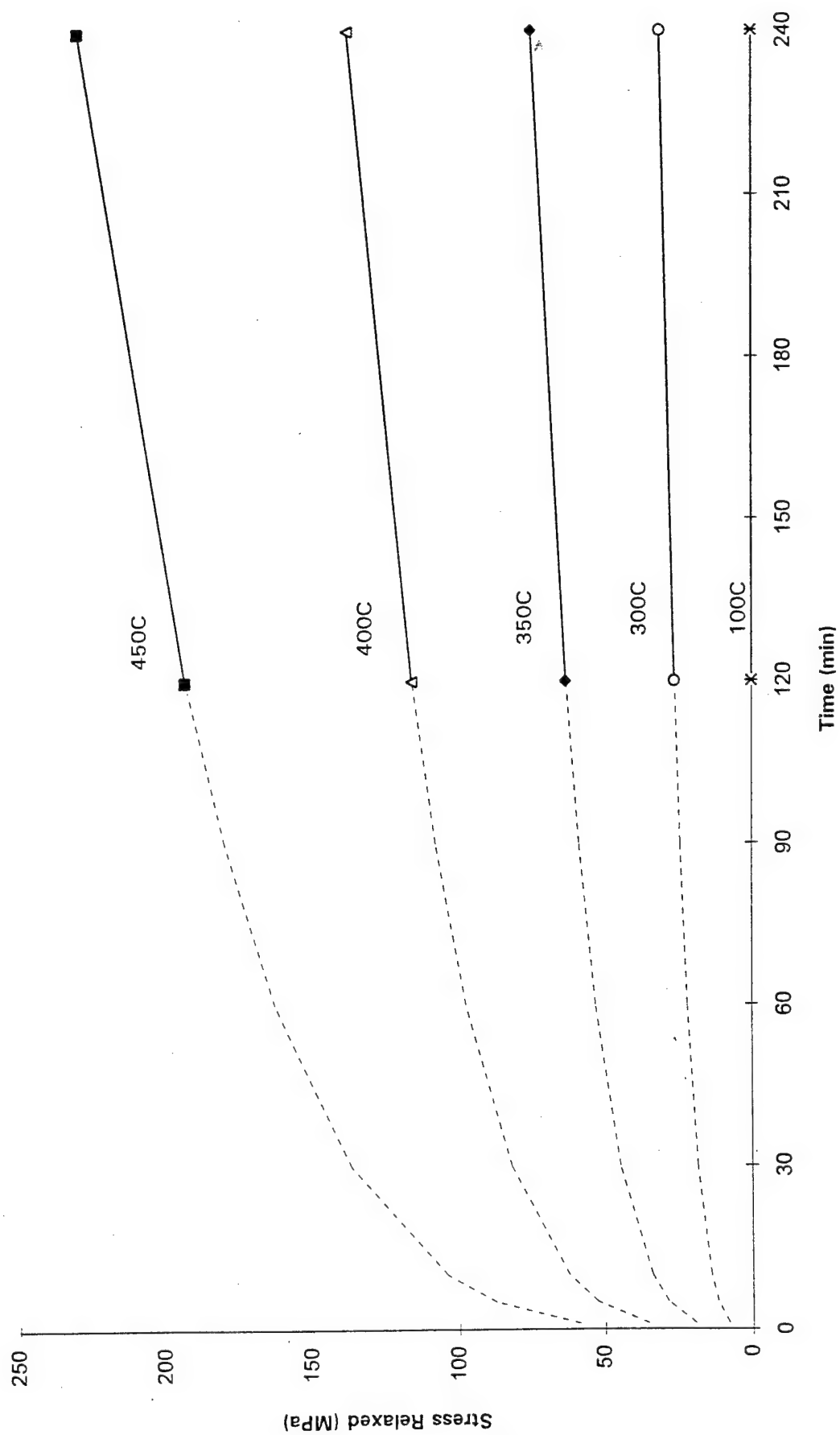


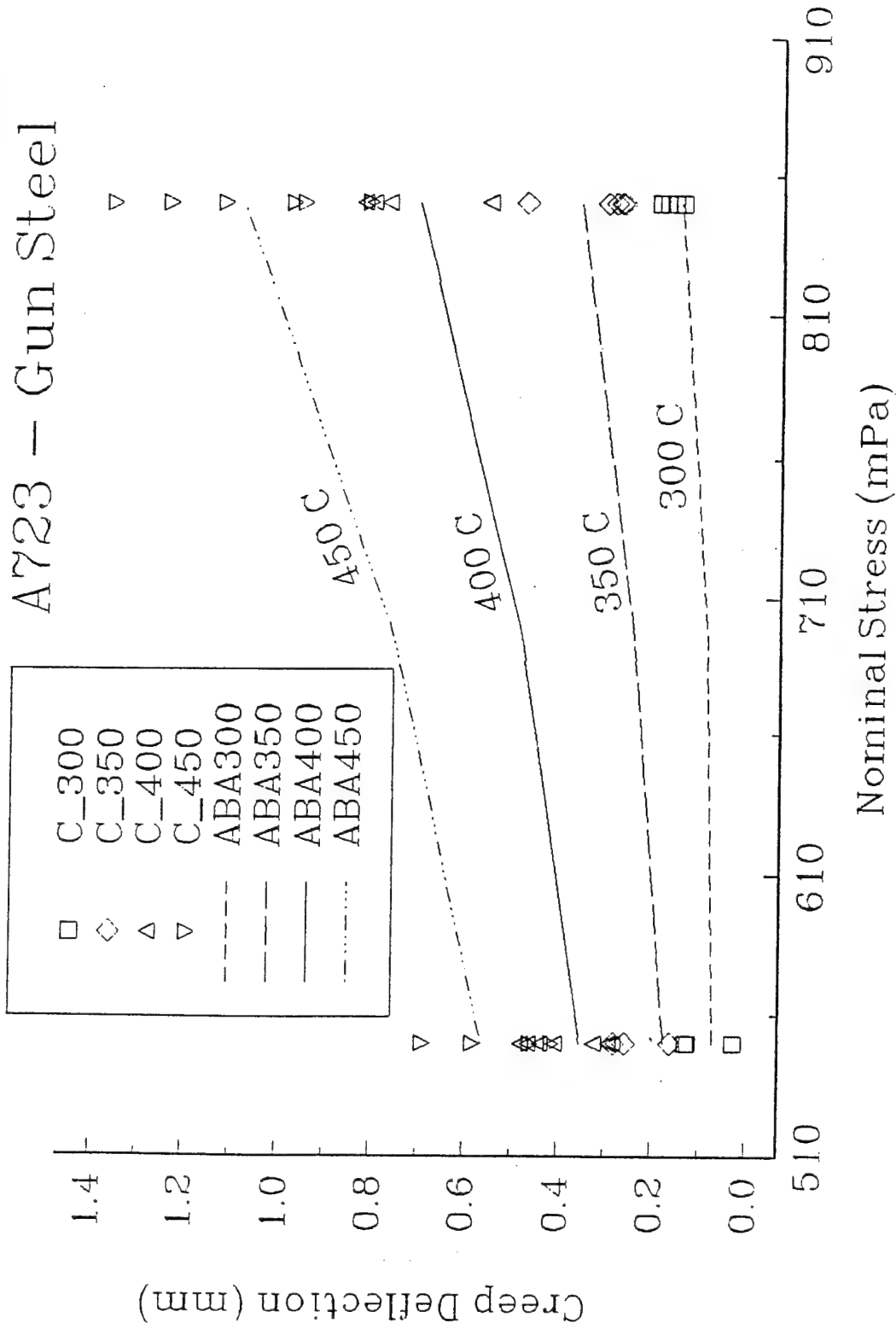
Figure 10. Stress relaxed as predicted by creep model

Creep Analysis

ASTM E328 - 86



A723 - Gun Steel



G. Peter O'Hara

Modeling + Simulation

Figure 11. Creep deflection vs. applied stress

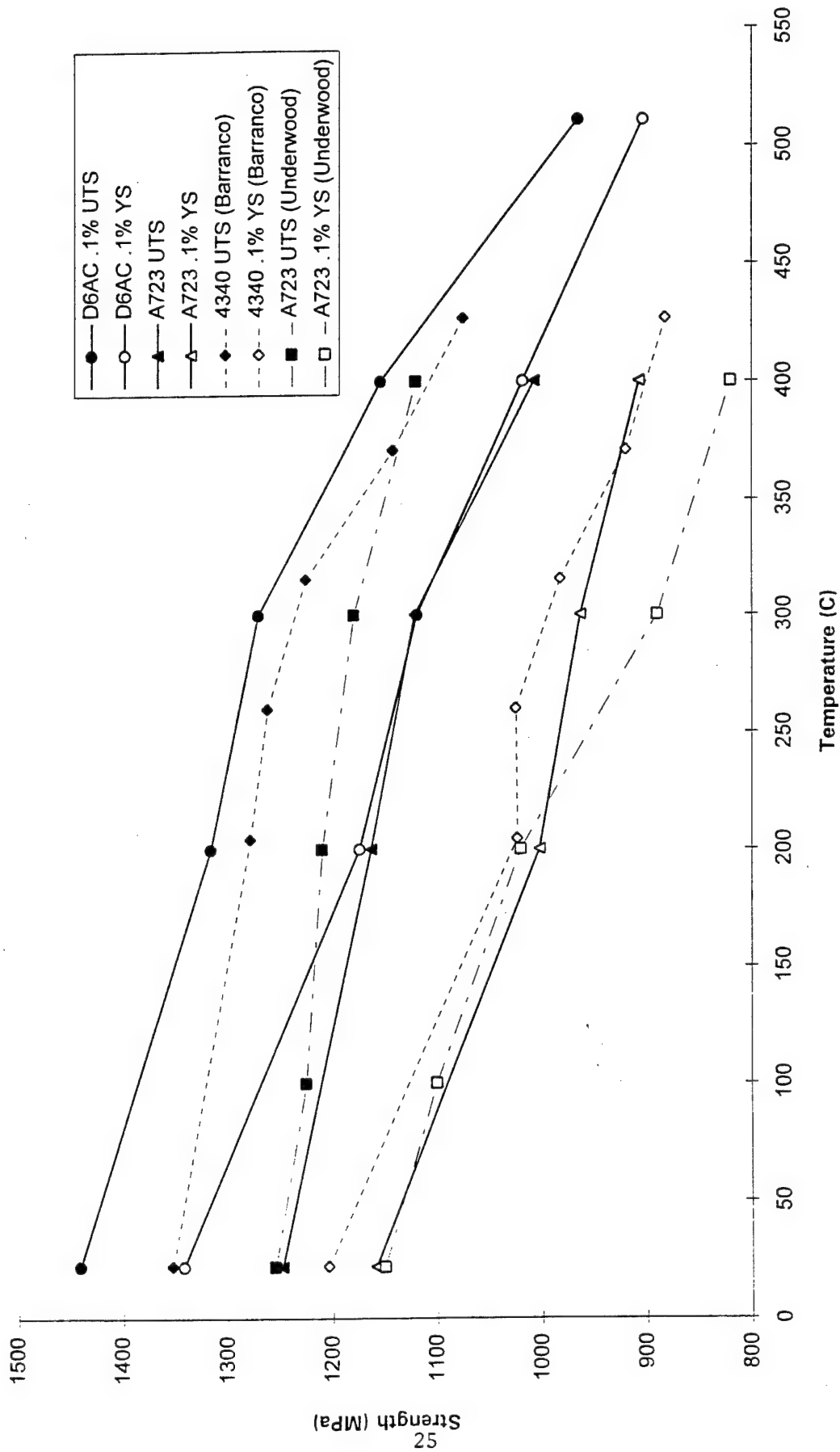


Figure 12. Strength vs. temperature

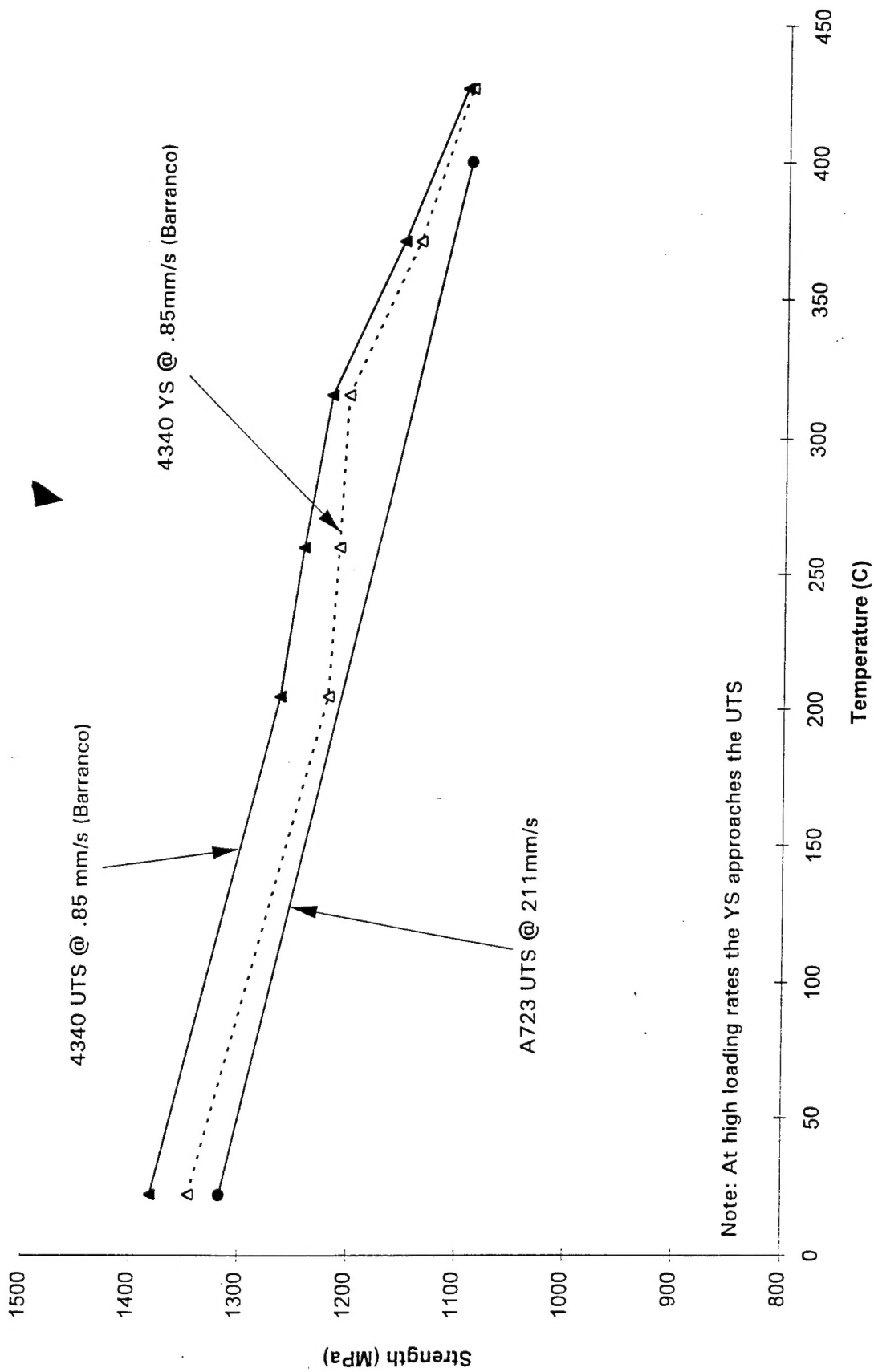


Figure 13. Effects of loading rate and temperature on strength

TECHNICAL REPORT INTERNAL DISTRIBUTION LIST

	<u>NO. OF COPIES</u>
CHIEF, DEVELOPMENT ENGINEERING DIVISION	
ATTN: AMSTA-AR-CCB-DA	1
-DB	1
-DC	1
-DD	1
-DE	1
CHIEF, ENGINEERING DIVISION	
ATTN: AMSTA-AR-CCB-E	1
-EA	1
-EB	1
-EC	1
CHIEF, TECHNOLOGY DIVISION	
ATTN: AMSTA-AR-CCB-T	2
-TA	1
-TB	1
-TC	1
TECHNICAL LIBRARY	
ATTN: AMSTA-AR-CCB-O	5
TECHNICAL PUBLICATIONS & EDITING SECTION	
ATTN: AMSTA-AR-CCB-O	3
OPERATIONS DIRECTORATE	
ATTN: SIOWV-ODP-P	1
DIRECTOR, PROCUREMENT & CONTRACTING DIRECTORATE	
ATTN: SIOWV-PP	1
DIRECTOR, PRODUCT ASSURANCE & TEST DIRECTORATE	
ATTN: SIOWV-QA	1

NOTE: PLEASE NOTIFY DIRECTOR, BENÉT LABORATORIES, ATTN: AMSTA-AR-CCB-O OF ADDRESS CHANGES.

TECHNICAL REPORT EXTERNAL DISTRIBUTION LIST

	<u>NO. OF COPIES</u>		<u>NO. OF COPIES</u>
ASST SEC OF THE ARMY RESEARCH AND DEVELOPMENT ATTN: DEPT FOR SCI AND TECH THE PENTAGON WASHINGTON, D.C. 20310-0103	1	COMMANDER ROCK ISLAND ARSENAL ATTN: SMCRI-SEM ROCK ISLAND, IL 61299-5001	1
DEFENSE TECHNICAL INFO CENTER ATTN: DTIC-OCF (ACQUISITIONS) 8725 JOHN J. KINGMAN ROAD STE 0944 FT. BELVOIR, VA 22060-6218	2	MIAC/CINDAS PURDUE UNIVERSITY 2595 YEAGER ROAD WEST LAFAYETTE, IN 47906-1398	1
COMMANDER U.S. ARMY ARDEC ATTN: AMSTA-AR-AEE, BLDG. 3022	1	COMMANDER U.S. ARMY TANK-AUTMV R&D COMMAND ATTN: AMSTA-DDL (TECH LIBRARY) WARREN, MI 48397-5000	1
AMSTA-AR-AES, BLDG. 321	1	COMMANDER	
AMSTA-AR-AET-O, BLDG. 183	1	U.S. MILITARY ACADEMY	
AMSTA-AR-FSA, BLDG. 354	1	ATTN: DEPARTMENT OF MECHANICS	1
AMSTA-AR-FSM-E	1	WEST POINT, NY 10966-1792	
AMSTA-AR-FSS-D, BLDG. 94	1		
AMSTA-AR-IMC, BLDG. 59	2	U.S. ARMY MISSILE COMMAND	
PICATINNY ARSENAL, NJ 07806-5000		REDSTONE SCIENTIFIC INFO CENTER	2
		ATTN: AMSMI-RD-CS-R/DOCUMENTS	
DIRECTOR		BLDG. 4484	
U.S. ARMY RESEARCH LABORATORY		REDSTONE ARSENAL, AL 35898-5241	
ATTN: AMSRL-DD-T, BLDG. 305	1		
ABERDEEN PROVING GROUND, MD		COMMANDER	
21005-5066		U.S. ARMY FOREIGN SCI & TECH CENTER	
		ATTN: DRXST-SD	1
DIRECTOR		220 7TH STREET, N.E.	
U.S. ARMY RESEARCH LABORATORY		CHARLOTTESVILLE, VA 22901	
ATTN: AMSRL-WT-PD (DR. B. BURNS)	1		
ABERDEEN PROVING GROUND, MD		COMMANDER	
21005-5066		U.S. ARMY LABCOM, ISA	
		ATTN: SLCIS-IM-TL	1
DIRECTOR		2800 POWER MILL ROAD	
U.S. MATERIEL SYSTEMS ANALYSIS ACTV		ADELPHI, MD 20783-1145	
ATTN: AMXSY-MP	1		
ABERDEEN PROVING GROUND, MD			
21005-5071			

NOTE: PLEASE NOTIFY COMMANDER, ARMAMENT RESEARCH, DEVELOPMENT, AND ENGINEERING CENTER,
BENÉT LABORATORIES, CCAC, U.S. ARMY TANK-AUTOMOTIVE AND ARMAMENTS COMMAND,
AMSTA-AR-CCB-O, WATERVLIET, NY 12189-4050 OF ADDRESS CHANGES.

TECHNICAL REPORT EXTERNAL DISTRIBUTION LIST (CONT'D)

	<u>NO. OF COPIES</u>		<u>NO. OF COPIES</u>
COMMANDER U.S. ARMY RESEARCH OFFICE ATTN: CHIEF, IPO P.O. BOX 12211 RESEARCH TRIANGLE PARK, NC 27709-2211	1	WRIGHT LABORATORY ARMAMENT DIRECTORATE ATTN: WL/MNM EGLIN AFB, FL 32542-6810	1
DIRECTOR U.S. NAVAL RESEARCH LABORATORY ATTN: MATERIALS SCI & TECH DIV WASHINGTON, D.C. 20375	1	WRIGHT LABORATORY ARMAMENT DIRECTORATE ATTN: WL/MNMF EGLIN AFB, FL 32542-6810	1

NOTE: PLEASE NOTIFY COMMANDER, ARMAMENT RESEARCH, DEVELOPMENT, AND ENGINEERING CENTER,
BENÉT LABORATORIES, CCAC, U.S. ARMY TANK-AUTOMOTIVE AND ARMAMENTS COMMAND,
AMSTA-AR-CCB-O, WATERVLIET, NY 12189-4050 OF ADDRESS CHANGES.
